Quaternary Research 80 (2013) 274–283

Contents lists available at ScienceDirect

Quaternary Research

journal homepage: www.elsevier.com/locate/yqres

Timing of advance and basal condition of the Laurentide Ice Sheet during the last glacial maximum in the Richardson Mountains, NWT

Denis Lacelle [a,*], Bernard Lauriol [a], Grant Zazula [b], Bassam Ghaleb [c], Nicholas Utting [d,e], Ian D. Clark [d]

[a] Department of Geography, University of Ottawa, Ottawa, Canada
[b] Department of Tourism and Culture, Government of Yukon, Whitehorse, Canada
[c] Centre de recherche en géochimie et géodynamique, GEOTOP, Université du Québec a Montréal, Montréal, Canada
[d] Department of Earth Science, University of Ottawa, Ottawa, Canada
[e] BGC Engineering Inc, Vancouver, BC, Canada

ARTICLE INFO

Article history:
Received 17 December 2012
Available online 16 July 2013

Keywords:
Laurentide Ice Sheet
Last glacial maximum
Ground ice
Richardson Mountains
Western Arctic

ABSTRACT

This study presents new ages for the northwest section of the Laurentide Ice Sheet (LIS) glacial chronology from material recovered from two retrogressive thaw slumps exposed in the Richardson Mountains, Northwest Territories, Canada. One study site, located at the maximum glacial limit of the LIS in the Richardson Mountains, had calcite concretions recovered from aufeis buried by glacial till that were dated by U/Th disequilibrium to 18,500 cal yr BP. The second site, located on the Peel Plateau to the east yielded a fossil horse (*Equus*) mandible that was radiocarbon dated to ca. 19,700 cal yr BP. These ages indicate that the Peel Plateau on the eastern flanks of the Richardson Mountains was glaciated only after 18,500 cal yr BP, which is later than previous models for the global last glacial maximum (LGM). As the LIS retreated the Peel Plateau around 15,000 cal yr BP, following the age of the Tutsieta phase, we conclude that the presence of the northwestern margin of the LIS at its maximum limit was a very short event in the western Canadian Arctic.

© 2013 University of Washington. Published by Elsevier Inc. All rights reserved.

Introduction

Previous chronological reconstructions of the northwest margin of the Laurentide Ice Sheet (LIS) have been controversial, with proposed ages for the all-time maximum advance ranging between ca. 30,000 to ca. 16,000 cal yr BP (Hughes et al., 1981; Rampton, 1982; Catto, 1986, 1996; Morlan, 1986; Vincent, 1989; Duk-Rodkin and Hughes, 1991; Lemmen et al., 1994; Duk-Rodkin et al., 1996; Duk-Rodkin and Lemmen, 2000; Dyke et al., 2002; Zazula et al., 2004, 2009a; England et al., 2009; Kennedy et al., 2010; Lauriol et al., 2010). Controversy has been perpetuated because of disagreements in radiocarbon ages obtained from various types of organic remains (bulk material and wood remains being much older than herb fragments; Kennedy et al., 2010). There is also disagreement between radiocarbon ages and other geochronological datasets, and a seeming lack of correlation between results from the unglaciated peripheries and formerly glaciated terrains (Hughes, 1972; Zazula et al., 2004; Kennedy et al., 2010). Much of the recent results advocate that the maximum advance of the LIS along its northwest margin is broadly correlative with the global LGM and occurred during Marine Oxygen Isotope Stage (MIS) 2 (Dyke et al., 2002; Clark et al., 2009). According to Clark et al. (2009), the onset of Northern Hemisphere deglaciation at 19,000 cal yr BP was induced by an increase in northern summer insolation. However, this general timing of deglaciation is inconsistent with recent stratigraphic and sedimentological work conducted near the headwaters the Eagle River basin, an unglaciated area west of the Richardson Mountains (Kennedy et al., 2010; Lauriol et al., 2010). In this area, radiocarbon ages from fluvial sediments indicate that the LIS reached its maximum extent and diverted the Peel River northwest to the unglaciated Old Crow, Bell and Bluefish basins as late as 18,000–16,000 cal yr BP (Fig. 1). As such, additional chronological data are required to help constrain the timing of the LIS advance along the Richardson Mountains better. In addition, little is known about the basal condition of LIS during its advance in the area. Beget (1987) inferred the presence of a warm-based LIS from reconstructed paleocontours of the ice-sheet surface, but this has yet been supported by other proxies. The basal condition of the LIS in the Richardson Mountains would influence subglacial drainage, permafrost thermal regime and ground ice conditions during the late Pleistocene.

This study presents new chronological data that further supports that the LIS reached its maximum extent along the Richardson Mountains relatively late, ca. 18,000–16,000 cal yr BP. The new ages consist of: i) U-series dating of carbonate concretions extracted from an aufeis buried by till and preserved in relict permafrost at the maximum position reached by the LIS; and ii) a radiocarbon date on a fossil horse (*Equus* sp.) mandible recovered on the floor of a thaw slump along a recessional margin position of the LIS on the Peel Plateau, NWT. The basal condition of the LIS during its advance during the LGM is derived from the $\delta^{18}O$ composition of carbonate concretions.

* Corresponding author.
E-mail address: dlacelle@uottawa.ca (D. Lacelle).

0033-5894/$ – see front matter © 2013 University of Washington. Published by Elsevier Inc. All rights reserved.
http://dx.doi.org/10.1016/j.yqres.2013.06.001

https://doi.org/10.1016/j.yqres.2013.06.001 Published online by Cambridge University Press

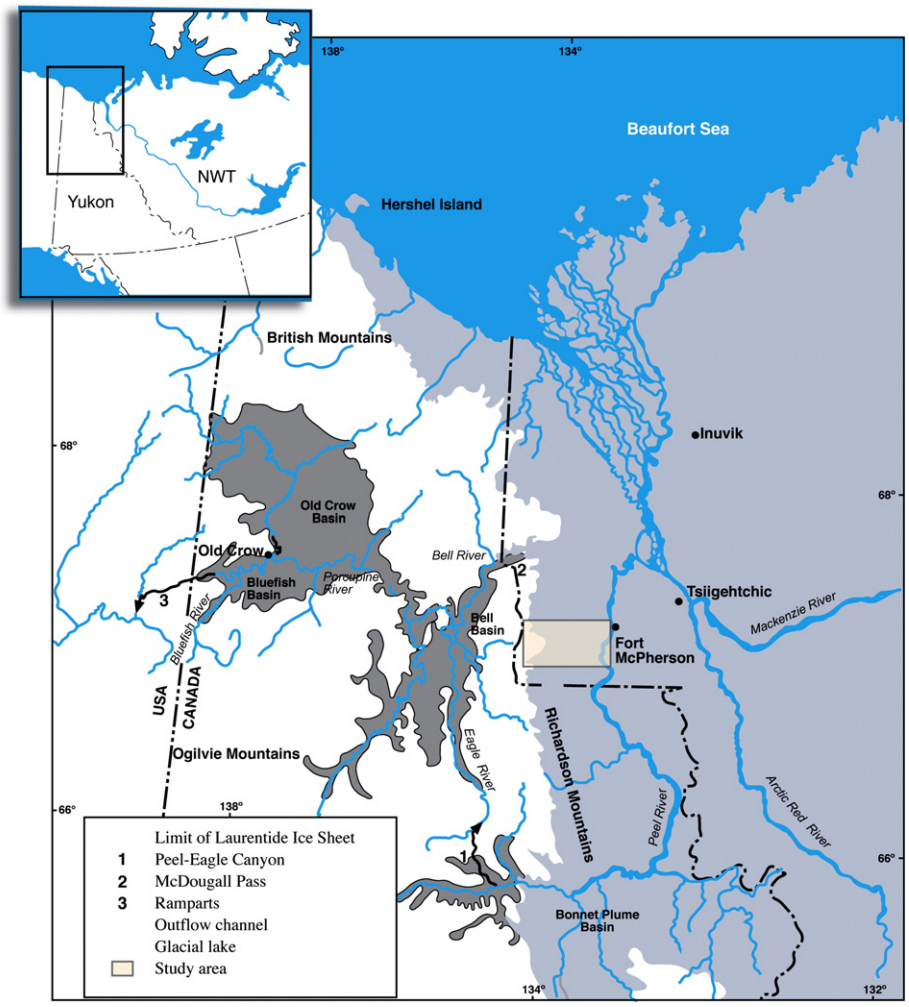

Figure 1. Map of northern Yukon Territory and northwestern Northwest Territories showing limit of Laurentide Ice Sheet and proglacial lakes in eastern Beringia. The study area, outlined in box with a star, is situated on the Peel Plateau along the Richardson Mountains, NWT, Canada.

Study sites

This study provides new data that help constrain the timing of advance and retreat of the LIS along the Richardson Mountains, NWT, as well as its basal condition. The new data are collected from two sites (Fig. 2). The first site (FM10; or Creek site) is situated at the maximum extent of the LIS, whereas the second site (FM3; or Melanie site) is situated along an unnamed standstill of the LIS and 3 km west of the Tutsieta Phase dated at 15,000 cal yr BP by Duk-Rodkin and Hughes (1995). According to Duk-Rodkin and Hughes (1995), the unnamed standstill is considered to be correlative with the Katherine Creek Phase in the Mackenzie Mountains and the Sabine Phase north of McDougall Pass. At both sites, material was recovered from the headwall and the floor of retrogressive thaw slumps.

The FM10, Creek site

The FM10 site (67°07.75′N; 135°55.74′W; 620 m asl) is located on the interfluve of a small topographic basin, about 20 km^2 in surface area, in the Richardson Mountains, NWT. A canyon 50 m deep dissects the basin in which flows a tributary of Vittrekwa Creek. The slopes of the canyon consist primarily of Devonian age shale (Norris, 1985). A veneer (10–15 m thick) of unconsolidated sediment associated with the late Pleistocene glaciation covers the bottom of the basin, which is surrounded by hills with summits exceeding 1000 m asl. According to Duk-Rodkin and Hughes (1992) and our own observations, the terminal limit of the LIS reached an elevation of about 650 m on the western slopes of the basin and 800 m on the eastern slopes. As the elevation of the topographic basin is around 600 m, a 100-to 300-m-thick layer of ice would have covered the area during the maximum glacial advance, a thickness that is consistent with estimates by Beget (1987). Glacial erratics, including numerous granite blocks originating from the Canadian Shield, are found in the creek bottom, which confirms the former presence of the LIS at the site and its surroundings.

The FM3, Melanie site

The FM3 site (67°15.19′N; 135°16.28′W; 380 m asl) is situated upstream of Dempster Creek (unofficial name), a small tributary of Stony Creek on the Peel Plateau, NWT. It is located 28 km east of the FM10 site, and therefore within 30 km from the maximum limit of the LIS. In this area, the local bedrock consists of shale of the Arctic River Formation (Norris, 1985). According to the surficial geology map (Duk-Rodkin and Hughes, 1992), the site is on a north–south orientated unnamed glacial standstill that developed during retreat or readvance of the LIS after the initial deglaciation. During this phase, meltwater drained north into McDougall Pass along an ice-marginal channel parallel to this recessional ice limit.

https://doi.org/10.1016/j.yqres.2013.06.001 Published online by Cambridge University Press

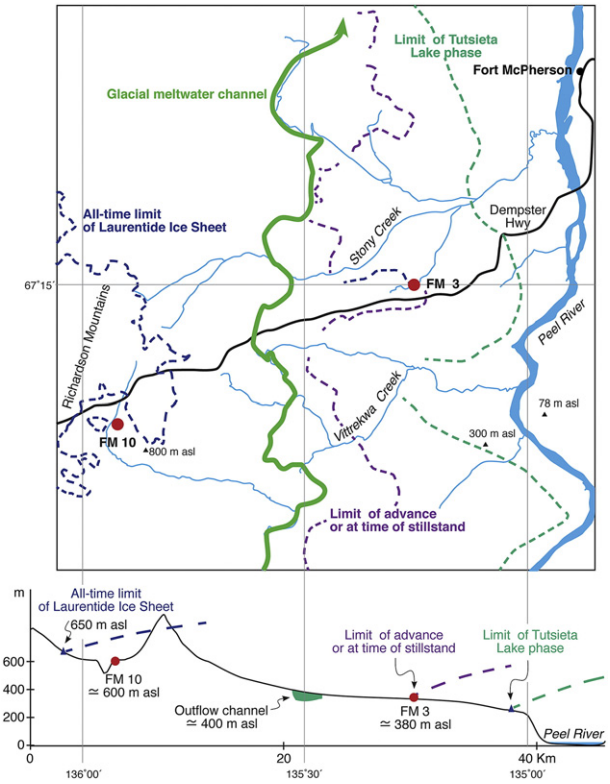

Figure 2. A) Map showing location of the two study sites (FM10 and FM3) in relation to the all-time limit of Laurentide Ice Sheet along the Richardson Mountains as well as the limits of the Tutsieta Phase and an unnamed standstill limit identified by Duk-Rodkin and Hughes (1992) on the Peel Plateau. B) Schematic topographic profile between the Richardson Mountains and the Peel River Valley, NWT, Canada and showing the location of the two study sites (FM10 and FM3) with the limit of the Laurentide Ice Sheet and the two glacial phases.

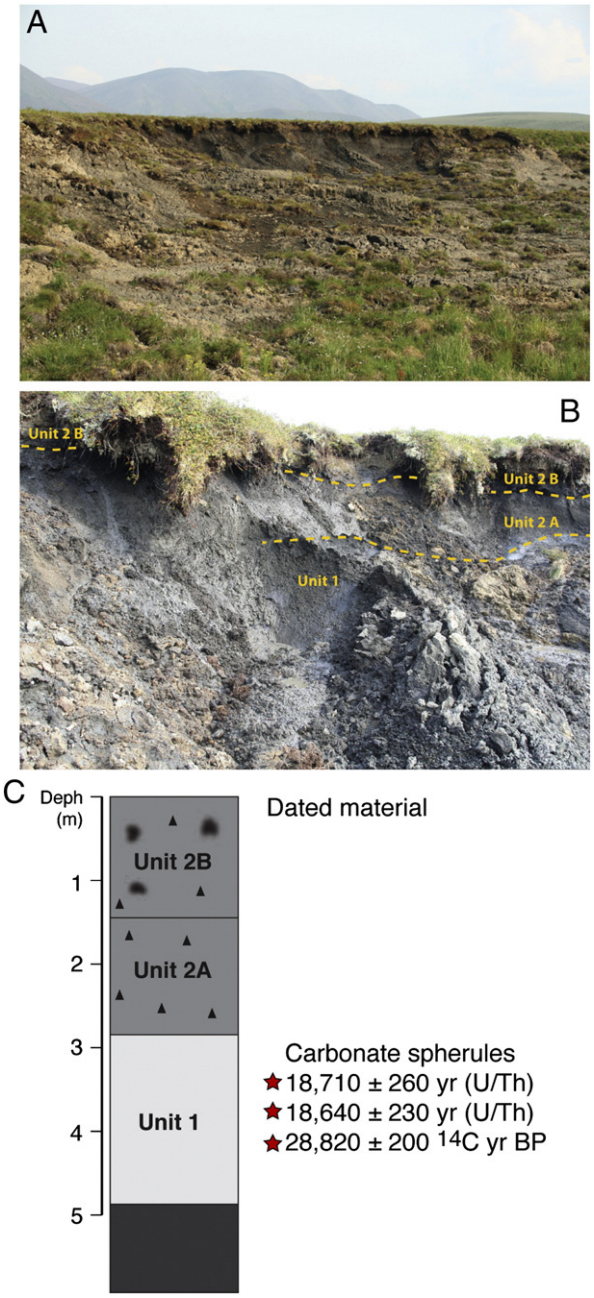

Figure 3. A) Field photograph showing retrogressive thaw slump at site FM10. B) View of the 3–5 m high headwall. The massive ground-ice exposure is indicated with an arrow. C) Schematic diagram of the units exposed in the headwall, $\delta^{18}O$ stratigraphy in the various units and location of dated material and associated ages.

Methodology

Sampling

At the FM10 site, sediments and ice-rich permafrost were sampled in summer 2009 from the headwall of a 3 ha hillslope retrogressive thaw slump (Fig. 3). In the 3–5 m high headwall, two stratigraphic units were observed: i) Unit 1 consisted of bubble-rich massive ice body of an undetermined thickness (the base being covered by slumped sediments); and ii) Unit 2 was a gray (5Y5/1) icy diamicton consisting of a sediment matrix with a few small pebbles, mostly shale. The thickness of this icy diamicton varied from 1 to 4 m as the contact between the two units was wavy. Back in the laboratory, a 30-kg block of the massive ice from Unit 1 was melted in a beaker covered by cellophane. Numerous tiny carbonate concretions were released from the ice and dated by the radiocarbon and uranium–thorium (U/Th) disequilibrium methods. The melting of the ice also revealed the presence of brown hairballs a few mm wide, most likely originating from a lemming-type mammal.

At the FM3 site, sediments and ground ice were sampled in summer 2010 and 2011 from a retrogressive thaw slump that covers about 2 ha and includes a headwall about 10 m high (Fig. 4). The headwall exposed a diamicton composed of pebbles and silty-clay mixed with ice. It is possible to distinguish a 6-m-thick lower debris-rich ice unit (Unit 1) that exhibits sub-horizontal wavy bedding parallel to the ground surface and an upper 4-m-thick icy diamicton unit (Unit 2). The latter forms two sub-units: the lower unit (Unit 2a) which has a reticulate ice structure and the upper unit (Unit 2b) containing pieces of peat, in a parallel-layered lenticular pattern which includes the active layer. The thickness of Unit 1 is a minimum, as the lower contact was not observed due to slumped material. The contact between the debris-rich ice (Unit 1) and the icy-diamicton (Unit 2) is sharp, irregular and undulating. Four samples were recovered from the FM3 site for radiocarbon dating: peat, wood and two fossil bones: i) a partial mandible of a horse, *Equus* sp.; and ii) a thoracic vertebra of a caribou, *Rangifer tarandus*. Both bones were recovered from the slump floor at the base of the headwall, whereas the pieces of wood and peat were collected in situ in the headwall. The piece of wood, 15 cm in diameter and over 20 cm in length, was emerging from the lower Unit 1 in a perpendicular orientation with the headwall, following an east–west axis. The peat was collected in Unit 2b. The bones and wood pieces are now curated at the Prince of Wales Northern Heritage Centre in Yellowknife, NWT.

https://doi.org/10.1016/j.yqres.2013.06.001 Published online by Cambridge University Press

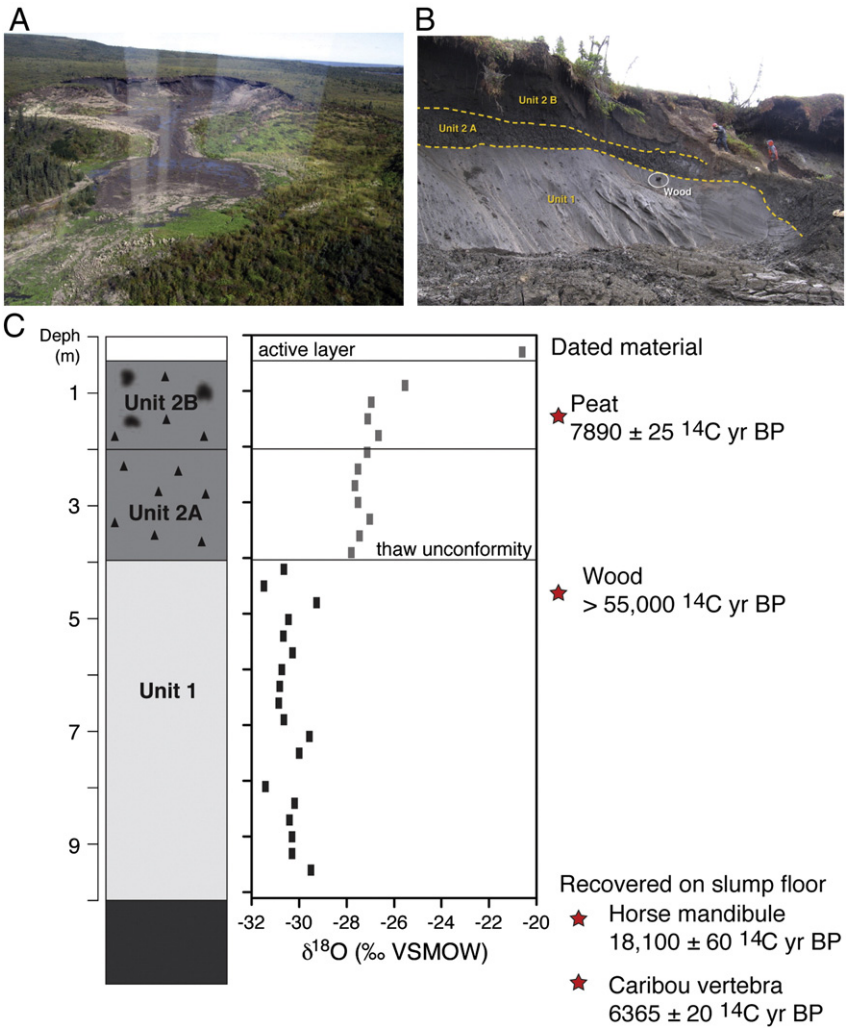

Figure 4. A) Field photograph showing retrogressive thaw slump at site FM3. B) View of the 10 m high headwall exposed in the thaw slump at site FM3 (note two persons for scale). C) Schematic diagram of the units exposed in the headwall and $\delta^{18}O$ stratigraphy in the various units. Isotopic discontinuities are observed below the modern active layer and at the paleo thaw unconformity. Also shown is the location of dated material and associated ^{14}C ages.

Analyses

At the FM3 site, thirty ice-rich sediment samples were collected, placed in sealed plastic bags and kept cold until laboratory analysis. At the FM10 site, two ground ice samples were collected from the icy diamicton unit and eleven from the underlying massive ground ice body. In the laboratory, the sediments were analyzed for grain-size distribution and geochemistry, whereas the melted ground ice samples were analyzed for stable water isotopes. In addition, a 30 kg block of ice was collected from the massive ice body at FM10 and kept frozen in a freezer until its analysis in the laboratory for occluded gases (O_2, N_2, Ar, Kr, Xe).

The grain-size distribution of the sediments was analyzed using a Microtrac S3500 laser particle-size analyser at the University of Ottawa and reported in three grain-size class: >63 μm sand, <63 μm silt >4 μm, <4 μm clay. The geochemistry of the sediments was analyzed by a Philips PW2400 X-ray Fluoresence with a Rh tube and 30 position sample changer at the University of Ottawa. Philips SuperQ/Quantitative and SemiQ/Qualitative software (ver. 2.1D) provided quantitative analysis of the geochemical composition of the samples.

To interpret the formation of the concretions contained in the body of massive ice at FM10 site, the origin of the ground ice was determined following the analysis of the stable water isotope and occluded gases. The analysis of the $\delta^{18}O$ and δD composition of the ground ice follows those described in St-Jean et al. (2011). The methods used to analyze the composition of the air trapped in the bubbles in the ice from the FM10 site follow those described by Cardyn et al. (2007) and Utting (2010).

The radiocarbon dating of the bones, wood and peat collected from FM3 were performed at the Keck Carbon Cycle Accelerator Mass Spectrometry Laboratory at the University of California, Irvine, USA. Procedures used in the preparation of the ultrafiltered (>30 kD) collagen are detailed in Beaumont et al. (2010). Detailed description of the combustion and graphitization protocols and the operation of the UCIAMS instrument are described in Beverly et al. (2010). The radiocarbon age of the horse mandible was calibrated to calendar years using the Intcal09 dataset (Reimer et al., 2009) at 95.4% confidence interval (OxCal v.4.1.7; Bronk Ramsey, 2009).

The carbonate concretions found in the massive ice unit at the FM10 site were extracted after melting the ice block samples. One liter of water provided approximately 80 mg of concretions with diameters less than 1 mm. The concretions were recovered by filtration on a 4-phi sieve (62 μm) and observed under a petrographic microscope and scanning electron microscope. Some concretions were also observed using an epifluorescence microscope to determine the potential presence of organic matter, whereas others were analyzed for $\delta^{18}O$ and $\delta^{13}C$ following methods described in Lacelle et al. (2006). Some concretions were radiocarbon dated by AMS at Beta Analytic Radiocarbon (calibrated to calendar years using the Intcal09 dataset; Reimer et al., 2009), while others were dated by TIMS measurements of the U/Th

https://doi.org/10.1016/j.yqres.2013.06.001 Published online by Cambridge University Press

disequilibrium methods at the GEOTOP (Universite du Québec à Montréal, QC) following methods described in Refsnider et al. (2012). Radiocarbon and U-series analyses were performed on bulk samples of carbonate concretions. Negligible amount of detrital fractions inside and outside the concretions as indicted by $^{230}Th/^{232}Th > 70$ were observed which are suitable conditions for U/Th dating (Hillaire-Marcel and Causse, 1989).

Overall, the three radiocarbon dates from the FM3 site and the ^{14}C and U/Th ages derived from the carbonate concretions contained in the massive ice at the FM10 site enables the development of the geochronology of the LIS along the Richardson Mountains, whereas the $\delta^{18}O$ composition of the carbonate spherule allows us to infer its basal condition.

Results and interpretations

The FM10 site

The headwall of the FM10 thaw slump shows two units (Fig. 3): the upper unit consists of an icy diamicton (Unit 2), whereas the lower unit consists of a body of massive ground ice (Unit 1). The icy diamicton contains clasts of shale and also ca. 5% granite pebbles originating from the Canadian Shield, suggesting that it consists of a till that was deposited when the LIS reached its maximum extent. X-ray fluorescence analysis supports a Canadian Shield source for the sediments, with high abundance of U and Th and <1% of carbonates (Table 1). Grain-size analysis shows that the icy till consists of a silty clay (6.9% sand; 67.5% silt; 25.6% clay). Analysis of two ground ice samples from the icy till yielded average $\delta^{18}O$ and δD values of −22.0‰ and −168.8‰, respectively (Fig. 5). These $\delta^{18}O$ and δD values are within the range of Holocene formed ground ice (Michel, 2011). As such, it is suggested that precipitation during the early Holocene warm period, a period when the thickness of the active layer was ca. 1.5 times thicker than today, infiltrated the thawed till (Burn, 1997). The aggradation of permafrost following this warm climate period resulted in the formation of intrasedimental ground ice with elevated $\delta^{18}O$ and δD values.

The lower massive ground ice unit (Unit 1) is composed of columnar ice crystals. The average $\delta^{18}O$ and δD composition is −29.1 ± 0.6‰ and −226.0 ± 2.4‰ (n = 11), respectively, and the results are distributed along a regression slope of 3.4 ($\delta D = 3.4\ \delta^{18}O - 125$; $r^2 = 0.74$) (Fig. 5). The massive ground ice contains many spherical and elongated air bubbles. The air bubbles reach a maximum length of 8 mm and have a tendency to form bubble trains. Occluded gas analysis yielded $\delta O_2/Ar$ and $\delta N_2/Ar$ ratios of −21.6 ± 1.7% and −14.8 ± 0.5%, respectively. The δAr/Xe value was −26 ± 6% and the δKr/Xe value was −8 ± 9%. These ratios are in between the ratios of atmospheric air (δAr/Xe: 0%, δKr/Xe: 0%) and air-equilibrated water at 0°C (δAr/Xe: −75.9%, δKr/Xe: −50.7%), indicating the ice may have formed from a mix of snow and liquid water (Utting, 2010).

The body of massive ground ice underlying the icy till has $\delta^{18}O$ values similar to Pleistocene-age ground ice in other localities in northwestern Canadian Arctic (Michel, 2011). However, it cannot consist of buried LIS because: i) the regression slope between δD and $\delta^{18}O$ and occluded gas analyses are more consistent with a freezing origin (i.e., Cardyn et al., 2007; Lacelle, 2011); and ii) the ice contains brown balls of hair probably of a lemming-type mammal. The latter rules out an intrusive-segregated ice origin, as it would be difficult to explain the transportation of balls of hair under a thermal and hydraulic gradient transport of water. Together, the elongated vertical ice crystals and

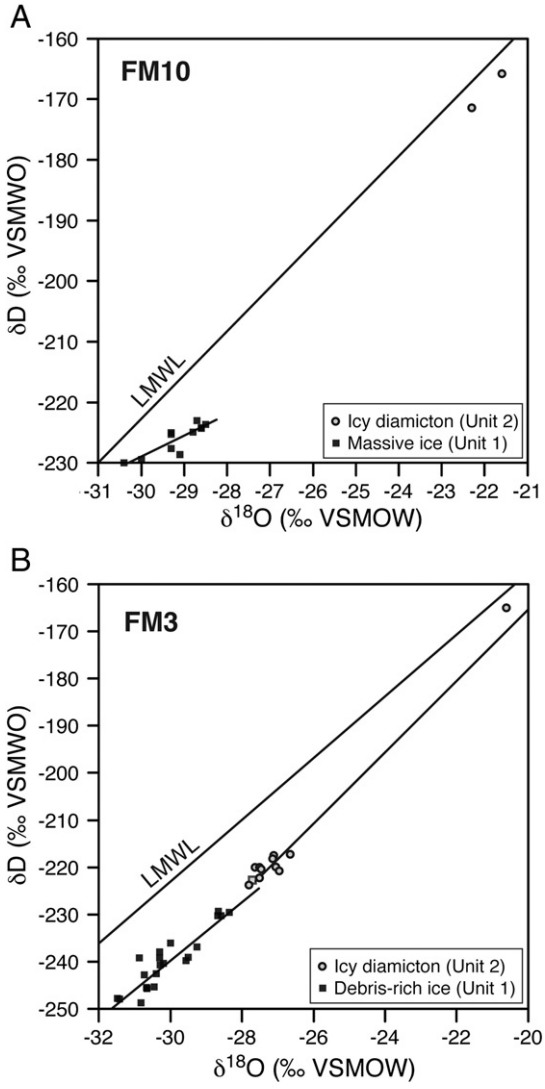

Figure 5. δD-$\delta^{18}O$ diagram of ice-bearing permafrost exposed in the headwalls. A) FM10 site, the ground ice $\delta^{18}O$ and δD values in Unit 1 are distributed along a regression slope of 3.4 ($\delta D = 3.4\ \delta^{18}O - 125$; $r^2 = 0.74$); B) FM3 site, the ground ice δD and $\delta^{18}O$ values in Unit 1 are distributed along a regression slope value of 6.4 ($\delta D = 6.4\ \delta^{18}O - 46.5$; $r^2 = 0.87$). LMWL = Local meteoric water line defined for Inuvik, NWT ($\delta D = 7.3\ \delta^{18}O - 3.37$; Lacelle, 2011).

Table 1
X-ray fluorescence results of till at the FM3 and FM10 sites, Richardson Mountains, NWT, Canada.

Sample ID	L.O.I. (%)	SiO_2 (%)	Al_2O_3 (%)	CaO (%)	K_2O (%)	MgO (%)	MnO (%)	Na_2O (%)	P_2O_5 (%)	Fe_2O_3(T) (%)	TiO_2 (%)	Sr (ppm)	Th (ppm)	U (ppm)
FM3 #9	11.99	61.66	12.87	1.17	2.339	1.66	0.046	0.70	0.265	5.410	0.747	135	18	11
FM3 #11	10.68	65.66	13.01	0.99	2.353	1.59	0.045	0.69	0.247	5.419	0.763	127	25	15
FM10 #11	11.64	62.92	13.45	1.08	2.418	1.66	0.045	0.70	0.225	5.623	0.794	126	19	12
FM10 #13	7.80	67.46	13.63	0.75	2.430	1.49	0.025	0.73	0.232	5.601	0.788	124	24	12
FM10 #14	11.11	59.19	17.30	0.80	3.034	1.88	0.041	0.49	0.247	6.486	0.839	138	17	<10
FM10 #15	12.26	58.90	17.18	0.88	3.024	1.89	0.044	0.50	0.245	6.444	0.834	144	25	14
FM10 #16	11.80	59.60	15.50	0.96	2.755	1.70	0.044	0.64	0.260	6.441	0.813	142	18	11
FM10 #17	10.07	60.28	17.68	0.88	3.121	1.95	0.045	0.50	0.252	6.603	0.857	148	20	12

https://doi.org/10.1016/j.yqres.2013.06.001 Published online by Cambridge University Press

freezing origin suggest that the body of massive ground ice consist of an aufeis that was buried by LIS till and preserved in permafrost. In the Richardson Mountains and adjacent northern Yukon, numerous aufeis are found (i.e., Lauriol et al., 1991) and a modern aufeis (James Creek aufeis) is situated less than 2 km from the FM10 site, suggesting that groundwater circulation necessary for the formation of aufeis exists in the area. The balls of hair could have been deposited on the surface of the aufeis by a small animal prior to its burial. The preservation of aufeis in relict permafrost is not unique to this area and has been described previously by Moorman and Michel (2000) in a proglacial setting on Bylot Island, NU, and by Froese et al. (2006) for the Klondike goldfields of west-central Yukon Territory. The interpretation that the massive ice unit consists of a buried aufeis also allows us to explain the presence of carbonate concretions released upon melting of the ice. The process of aufeis aggradation is associated with the production of mineral precipitates within the ice-layers by solute expulsion during freezing (Clark and Lauriol, 1997; Hall, 1980; Pollard, 2005; Lacelle et al., 2006). The most common minerals precipitated during aufeis growth are calcite ($CaCO_3$), gypsum ($CaSO_4 \cdot 2H_2O$), halite (NaCl) and ikaite ($CaCO_3 \cdot 6H_2O$). As such, it is suggested that the carbonate concretion formed in situ during aufeis aggradation and their age would provide a limiting maximum age for the advance of the LIS in the area.

Scanning electron microscope analyses show that the concretions released from the ice are composed of individual layers of tiny rhombroedral calcite crystals (Fig. 6), which is consistent with the minerals precipitated during aufeis formation. Since some of the concretions demonstrated epifluorescene, it is possible that they also contain a small amount of organic matter. The carbonate concretions are rich in U (ca. 40 ppm) and contain no detrital sediment (i.e., quartz, feldspars; this indicates that there was no thorium present in the samples at the time of precipitation). The $\delta^{18}O$ and $\delta^{13}C$ composition of the carbonate concretion yielded values of −24.9 and −8.3‰ VPDB, respectively. A comparison of $\delta^{18}O$ and $\delta^{13}C$ composition with various types of cryogenic carbonates indicate that their values are slightly more depleted than those obtained from modern cryogenic aufeis calcite in northern Yukon and NWT in similar geological units

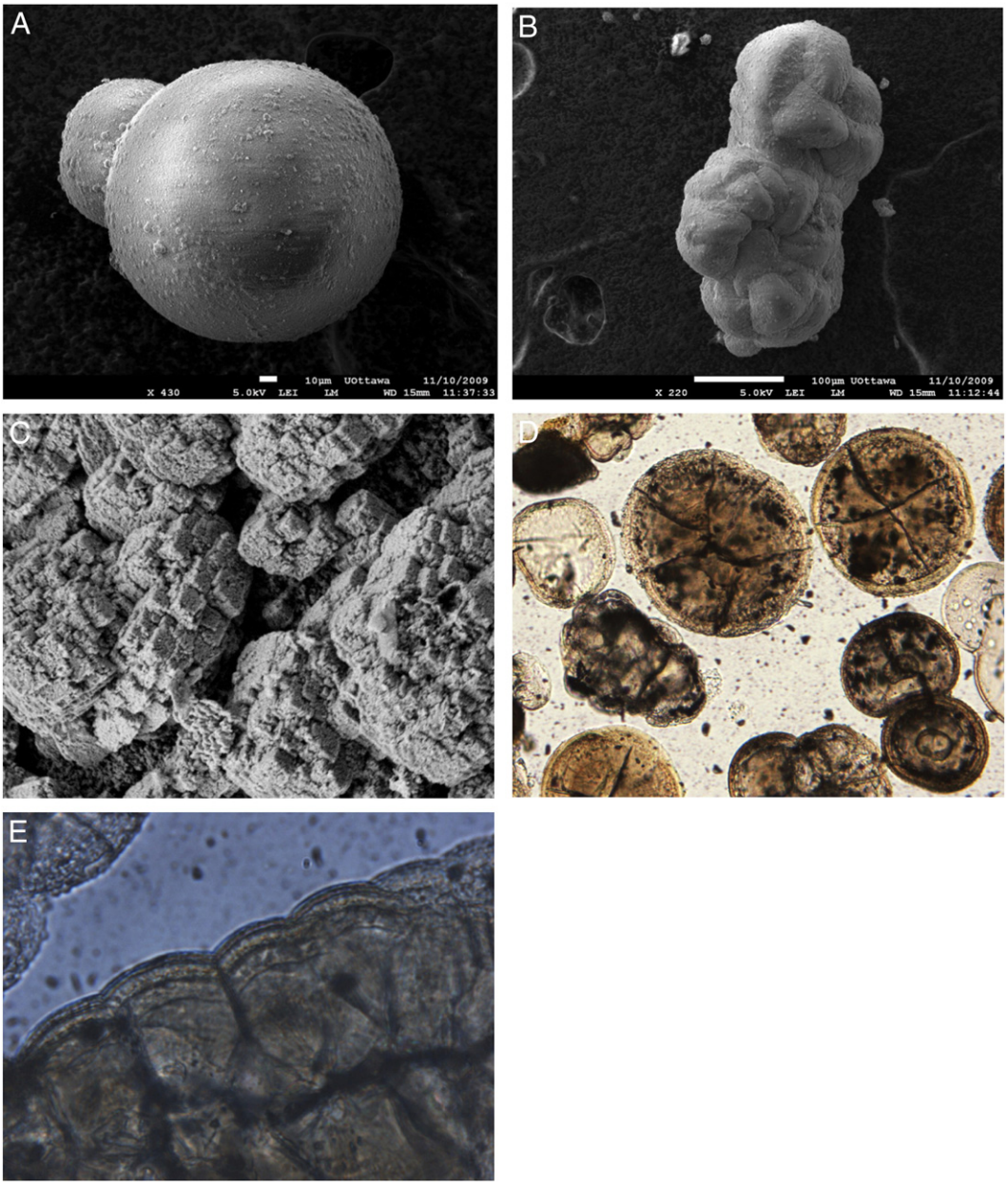

Figure 6. A–B) Concretions observed under scanning electron microscope; C) surface of one of the concretions examined under scanning electron microscope; D) concretions observed under petrographic microscope; E) close-up of edge of concretion observed under petrographic microscope.

https://doi.org/10.1016/j.yqres.2013.06.001 Published online by Cambridge University Press

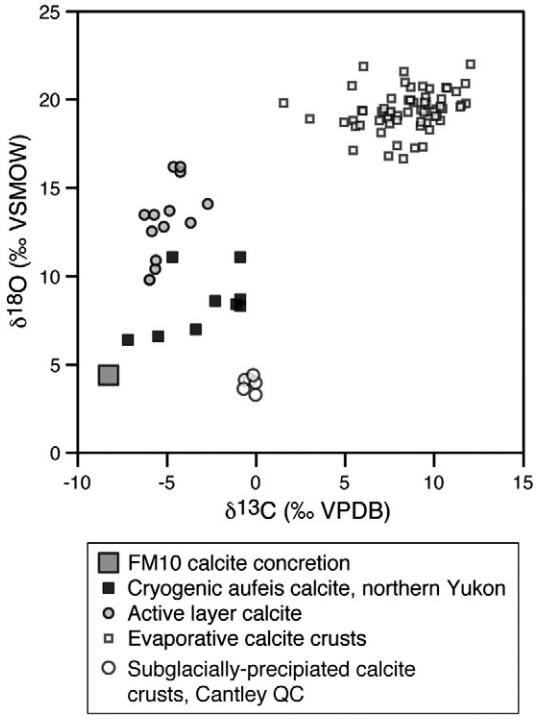

Figure 7. $\delta^{18}O$ and $\delta^{13}C$ composition of carbonate concretion retrieved from the body of massive ground ice (Unit 1) at FM10 compared to modern-day cryogenic aufeis calcite, active layer calcite crusts, evaporative calcite crusts and Pleistocene-age subglacially precipitated calcite crusts.
Data from Lacelle (2007).

(Fig. 7). A radiocarbon date from one of the carbonate concretion yielded an age of 28,820 ± 200 ^{14}C yr BP (Table 2). Two U/Th analyses performed on separate concretions yielded ages of 18,250 ± 250 yr and 18,639 ± 250 yr, respectively (Table 3). The radiocarbon age obtained from the carbonate concretion is most likely too old because the dissolved carbon from which the carbonate spherule formed most likely originates from dissolution of near ^{14}C-free carbonates. This was documented in Lacelle et al. (2006) where the ^{14}C dating of modern cryogenic aufeis calcite yielded ^{14}C activity of 44% modern carbon and ^{14}C ages near 6500 ^{14}C yr BP. However, since the dated material is rich in uranium, values of 40 ppm, this ensures that the U/Th result is accurate. As a result, we assume that the U/Th ages indicate the age of the concretions at the time of their precipitation in the growing aufeis. Therefore, the study site was most likely situated in a proglacial setting at 18,500 cal yr BP and the LIS only reached its maximum extent at or after 18,500 cal yr BP, which is after the onset of deglaciation for much of the Northern Hemisphere (i.e., 19,000 cal yr BP; cf. Clark et al., 2009).

Table 3
Uranium–thorium ages of carbonate concretions collected from the body of massive ground ice at the FM10 site, Richardson Mountains, NWT, Canada.

Sample ID	^{230}Th/^{234}U	^{234}U/^{238}U	Calendar age, yr
Concretion 1	0.1592 ± 0.0020	1.7421 ± 0.0163	18,710 ± 260
Concretion 2	0.1587 ± 0.0018	1.7722 ± 0.0124	18,640 ± 230

The FM3 site

In the headwall of the thaw slump (Fig. 4), it is possible to distinguish a lower debris-rich ice unit (Unit 1) that exhibits sub-horizontal wavy bedding parallel to the ground surface and an upper icy diamicton unit (Unit 2). The latter forms two sub-units: the lower unit (Unit 2a) which has a reticulate ice structure and the upper unit (Unit 2b) containing pieces of peat, in a parallel-layered lenticular pattern which includes the contemporary active layer. The sediment collected in the headwall of Unit 1 is composed of silty clay (64% silt, 29% clay and 7% sand; n = 24), which make up only half the volume, the other half being occupied by ice. Only a few pebbles (granite and gneiss: 13%; red sandstone and limestone: 2%; shale, chert and sandstone: 87%) were observed. Following the geochemical analyses, SiO_2 (61%) and Al_2O_3 (13%) are dominant, whereas similar to the FM10 site, the abundance of CaO is low (Table 1). The ground ice in Unit 1 has low $\delta^{18}O$ values (−31.5 to −27.7‰; n = 25) and in a δD-$\delta^{18}O$ diagram, the samples are distributed along a regression slope value of 6.4 ($\delta D = 6.4\ \delta^{18}O - 46.5$; $r^2 = 0.87$) (Fig. 5). In the overlying Unit 2, the ground ice has higher $\delta^{18}O$ values, reaching a maximum value of −20.6‰ in the modern active layer (Fig. 4).

The wood (PWNHC 2010-9.3) from Unit 1 yielded a radiocarbon age greater than 55,000 ^{14}C yr BP (Table 2). This age is consistent with other radiocarbon dated wood and macrofossils of woody taxa recovered along glacial margins of the western Arctic (Hopkins and Smith, 1981; Kennedy et al., 2010). Most of the infinite radiocarbon ages on wood (mainly *Picea*) from this region suggest they are reworked from last interglacial deposits and incorporated into alluvial and glacial deposits and remain well preserved in the permafrost. Binocular examination and loss-on-ignition of sediments that contained the wood did not reveal any additional organic matter, suggesting the wood piece was excavated from older sediments in the glacier forefront and preserved in the glacial till. The fact that the wood has not been destroyed by the glacier is probably related to the silty nature of the sediment from which it was recovered.

The peat that was collected in the upper organic-rich diamicton (Unit 2b) is Holocene in age (7890 ± 250 ^{14}C yr BP; Table 2). The peat was most likely incorporated into the sediments during permafrost degradation and solifluction associated with warm and humid climates of the early Holocene of the western Arctic (i.e., Kaufman et al., 2004). These diamicton sediments have similar characteristics as those containing the piece of wood. Further, the $\delta^{18}O$ values of the

Table 2
Radiocarbon ages of various materials collected at the FM3 and FM10 sites, Richardson Mountains, NWT, Canada. Note: N.M. = not measured. The radiocarbon ages were calibrated to calendar years using the Intcal09 dataset (Reimer et al., 2009).

Site	Material	Identification (specimen number)	^{14}C yr BP	cal yr BP	$\delta^{13}C$ (‰)	Laboratory number
FM3	Left partial mandible	Equus sp. (PWNHC 2010.9.1)	18,100 ± 60	20,070 to 19,390	−21.0	UCIAMS-81875
FM3	Thoracic vertebra	Rangifer tarandus (PWNHC 2010.9.2)	6365 ± 20	7310 to 7270	−20.7	UCIAMS-81876
FM3	Wood	Unknown species (PWNHC 2010.9.3)	>55,000		N.M.	UCIAMS-81608
FM3	Peat		7890 ± 25	8655 to 8630	N.M.	UCIAMS-84608
FM10	Carbonate concretion		28,820 ± 200	33450 to 33100	−8.8	Beta 271,111

https://doi.org/10.1016/j.yqres.2013.06.001 Published online by Cambridge University Press

ground ice in Unit 2b is close to −23‰, which is characteristic of the average isotopic values of early Holocene age ground ice in the western Canadian Arctic (Michel, 2011).

Collagen extracted from the two bones collected at the base of the headwall yielded a radiocarbon age of 6365 ± 20 ^{14}C yr BP for the caribou vertebra and 18,100 ± 60 ^{14}C yr BP (20,070 and 19,390 cal yr BP) for the horse mandible (Table 2). The original stratigraphic position of the bones in the headwall is uncertain, nevertheless we can assume that the caribou vertebra originates from Unit 2, the organic-rich diamicton that contained the peat dated at 7890 ± 250 ^{14}C yr BP, whereas the horse mandible likely originates from the lower Unit 1, which included the piece of wood.

Figure 8. Photograph of the horse mandible (*Equus* sp.) dated to ~19,700 cal yr BP. The mandible was recovered on the slump floor of site FM3. The scale bar measures 2.5 cm in length.

Discussion

Timing of the Last Glacial Maximum of the LIS along the Richardson Mountains, NWT

The two U/Th dates on the calcite concretions (18,710–18,640 yr) and the AMS radiocarbon date on the horse mandible (20,070–19,390 cal yr BP) provide important ages to constrain the timing of the maximum glacial limit of the LIS along the Richardson Mountains. The ^{14}C age from the piece of wood in Unit 1 at the FM3 site (>55,000 ^{14}C yr BP) is discarded because it is most likely associated with reworked material from the last interglacial and incorporated into glacial sediments.

Together, the three ages and the assumption that the Laurentide till buried the aufeis suggest that the Richardson Mountains were ice-free around 19,700 cal yr BP as horses were present in the area. The LIS reached its maximum extent along the Richardson Mountains only after about 18,500 cal yr BP, corresponding to the burial of the aufeis by LIS till. A late MIS 2 advance of the LIS along the Richardson Mountains is consistent with ^{14}C ages from fluvial sediments in the Old Crow, Bell and Bluefish basins in unglaciated Yukon Territory (Kennedy et al., 2010; Lauriol et al., 2010) and with ^{36}Cl ages in the Mackenzie Mountains that indicate that the LIS left the site at about 19,000 ± 1900 yr (Duk-Rodkin et al., 1996). Our results also support other glacial chronologies from the Yukon Coastal Plain (Fritz et al., 2012), Tuktoyaktuk Peninsula (Bateman and Murton, 2006; Murton et al., 2007) and the western Arctic Archipelago (England et al., 2009) that the maximum advance of the LIS in northwest Canada occurred during the late MIS 2. However, this chronology of a late MIS 2 age advance of the LIS in the Richardson Mountains is in disagreement with chronological studies conducted in the 1980s (i.e., Hughes et al., 1981; Catto, 1986; Schweger and Matthews, 1991). These studies inferred a much earlier advance of the LIS, 35,000–22,000 cal yr BP, and the chronology was established on dating bulk organic remains. But as Kennedy et al. (2010) pointed out, ^{14}C ages from bulk material are most likely too old due to the incorporation of last interglacial woody remains, as evidenced from the piece of wood recovered from Unit 1 at the FM3 site that yielded an infinite radiocarbon age.

As the Tutsieta Phase, dated at 15,000 cal yr BP by Duk-Rodkin and Hughes (1995), is located at 40 km east of the FM10 site and 3 km east of the FM3 site, our results suggest that the LIS covered the Peel Plateau for a maximum of 2000–3000 yr. The timing of a short-lived maximum glacial extent along the Richardson Mountains is supported by steppe bison (*Bison priscus*) remains radiocarbon dated to 13,565–13,810 cal yr BP from nearby Tsiigehtchic, 40 km east of the Peel Plateau (Zazula et al., 2009b). Further, based on optically stimulated luminescence ages from eolian sands, Murton et al. (2007) suggested that deglaciation along Tuktoyaktuk Peninsula began between 16,000 and 14,000 cal yr BP. This suggests a synchronous and late MIS 2 deglaciation along the northwest section of the LIS margin.

The new ages support the model that the northwest margin of the LIS reached its maximum position during late stage of MIS 2 (Dyke et al., 2002), later than the proposed global LGM by Clark et al. (2009). Clark et al. (2009) pointed out that the onset of deglaciation in the Northern Hemisphere that occurred between 20,000 and 19,000 cal yr BP and was induced by an increase in summer insolation, corresponding to an abrupt rise in sea level. Our results indicate that the LIS most likely reached its maximum extent in the Richardson Mountains between 18,500 and 15,000 cal yr BP. Although it is not certain why the northwest LIS margin advanced to its maximum position a few millennia after the global LGM (sensu Clark et al., 2009), we suggest that sea-level rise and increased opening of the Arctic Ocean along the Beaufort Sea coastline during the period of increased summer insolation provided a local source of moisture and enabling a rapid advance of the LIS in the Richardson Mountains and surrounding areas (i.e., Tuktoyaktuk Peninsula and western Arctic Archipelago). The increased summer insolation most likely resulted in higher evaporation rates, which would allow for increased precipitation and an advance of the LIS. Alternatively, a warm-based LIS (see section below) may have experienced a rapid advance as it moved over the soft deformable sediments in the Mackenzie Delta, as it was suggested for the Hudson Bay lowland (Vincent and Hardy, 1979).

Basal condition of the LIS in the Richardson Mountains, NWT

The basal condition of the LIS can be inferred from the $\delta^{18}O$ composition of the buried aufeis ice and carbonate spherules at FM10 site. Aufeis in a proglacial setting have been described on Bylot and Baffin islands (Moorman and Michel, 2000; Lacelle et al., 2006). In such an environment, the warm-based condition beneath the glacier allows for subglacial meltwater that discharges to the surface as it encounters impervious frozen ground near the terminus of the glacier. Considering that the exposure of the FM10 site is situated along an interfluve and not in a valley bottom, as observed for modern day aufeis, we can assume that the buried aufeis formed from subglacial meltwater discharging beneath a warm-based LIS and not from deep groundwater. Therefore, the $\delta^{18}O$ measurements of the aufeis ice and carbonate precipitates within the ice layers can provide an indication of the $\delta^{18}O$ values of the LIS subglacial meltwater.

At the FM10 site, the aufeis ice yielded an average $\delta^{18}O_{VSMOW}$ value of −29.1 ± 0.6‰, whereas the carbonate spherules yielded a $\delta^{18}O_{VPDB}$ value of −24.9‰. The $\delta^{18}O$ composition of the water from which the carbonate precipitated can be calculated by converting the $\delta^{18}O_{VPDB}$ to the $\delta^{18}O_{VSMOW}$ scale (Coplen et al., 1983) and using the temperature dependent fractionation factor between calcite and water at 0°C ($\varepsilon^{18}O$ $CaCO_3$–H_2O = 34.4‰; Bottinga, 1968). This calculation indicates that the carbonate spherules precipitated from water with a $\delta^{18}O_{VSMOW}$ composition of −29.2‰, similar to the average $\delta^{18}O$ of the aufeis ice (−29.1 ± 0.6‰).

A warm-based LIS in the Richardson Mountains during the LGM would largely affect the permafrost thermal regime, with thaw beneath the ice sheet. This condition would allow for groundwater

https://doi.org/10.1016/j.yqres.2013.06.001 Published online by Cambridge University Press

movement in the thawed ground. Following the retreat of the LIS, permafrost aggradation would result in the formation of segregated-intrusive ground ice. This type of ground ice was described from the Willow River watershed, ca 100 km north of the FM10 site, and the ground ice had $\delta^{18}O$ values ranging between −30 and −27‰ (i.e., Lacelle et al., 2004), similar to that inferred for the subglacial meltwater. This observation does not preclude other types of late Pleistocene age ground ice in the area, such as buried aufeis as described in this study or buried glacial ice.

Eastern Beringia habitat

The radiocarbon dated horse mandible from the FM3 site (Fig. 8) demonstrates that the Peel Plateau was ice-free around 19,700 cal yr BP. As such, during this period, the area comprised the easternmost edge of Beringia, the unglaciated arctic biotic refugium that stretched from Siberia to the west Arctic of Canada. Our new findings indicate that horses traversed these alpine regions of the northern Cordillera and occupied the eastern flanks of the Richardson Mountains during late MIS 2, within a climate certainly characterized by extreme cold and aridity. Horses are obligate grazers and are able to sustain themselves on abundant low-quality winter grassy vegetation that would have dominated the landscape for much of the year within this region bordering the continental ice sheet (Guthrie and Stoker, 1990). This further reinforces paleontological results obtained from other areas such the Beaufort Sea coastal plain (Guthrie and Stoker, 1990; Zazula et al., 2009a), Mackenzie Delta and southwest Arctic Archipelago (Harington, 1990) and northern Yukon (Burke and Cinq-Mars, 1989; Harington and Cinq-Mars, 1995), which indicate that mammals capable of persisting in the seemingly most dry and cold habitats, such as horses and saiga antelope (*Saiga tatarica*), were the most successful members of the faunal community along the periphery of Beringia during the LGM.

Conclusion

This study presents new ages for the northwest LIS glacial chronology from material recovered from two retrogressive thaw slumps exposed along the Richardson Mountains, NWT, Canada. One study site, located at the maximum glacial limit of the LIS in the Richardson Mountains, had calcite concretions recovered from a buried aufeis which we dated by U/Th disequilibrium to 18,500 cal yr BP. The second site, located on the Peel Plateau to the east yielded a fossil horse (*Equus* sp.) mandible that was radiocarbon dated to ~19,700 cal yr BP. These data indicate that the Peel Plateau on the eastern flanks of the Richardson Mountains was glaciated only after 18,500 cal yr BP, which is later than previous models for the global LGM. As the ice sheet retreated the Peel Plateau at 15,000 cal yr BP, following the age of the Tutsieta Lake phase moraine, we conclude that the presence of the LIS at its maximum limit was a very short event in this area.

Acknowledgments

This work was supported by NSERC Discovery and Northwest Territories Cumulative Impact Monitoring Program (NWT-CIMP) grants, with logistical support provided by a Polar Continental Shelf Project (PCSP) and Northern Scientific Training Program (NSTP). We thank John Southon of the Keck Carbon Cycle Accelerator Mass Spectrometry Laboratory for his continued excellence with radiocarbon dating of Pleistocene bones from northern Canada. We thank the two reviewers (D. Froese and A. Duk-Rodkin) as well as editors A. Gillespie and L. Owens for their constructive comments on the manuscript.

References

Bateman, M.D., Murton, J.B., 2006. The chronostratigraphy of Late Pleistocene glacial and periglacial aeolian activity in the Tuktoyatuk Coastlands, NWT, Canada. Quaternary Science Reviews 25, 2552–2568.
Beaumont, W., Beverly, R., Southon, J.R., Taylor, R.E., 2010. Bone preparation at the KCCAMS Laboratory. Nuclear Instruments and Methods in Physics Research B268, 906–909.
Beget, J., 1987. Low profile of the northwest Laurentide map sheets. Arctic and Alpine Research 19, 81–87.
Beverly, R.K., Beaumont, W., Tauz, D., Ormsby, K.M., von Reden, K.F., Santos, G.M., Southon, J.R., 2010. The Keck Carbon Cycle AMS Laboratory, University of California Irvine: status report. Radiocarbon 52 (2), 301–309.
Bottinga, I., 1968. Calculation of fractionation factors for carbon and oxygen exchange in the system calcite–CO_2–water. Journal of Physical Chemistry 72, 800–808.
Bronk Ramsey, C., 2009. Bayesian analysis of radiocarbon dates. Radiocarbon 51 (1), 337–360.
Burke, A., Cinq-Mars, J., 1989. Paleoethological reconstruction and taphonomy of *Equus lambei* from the Bluefish Caves, Yukon Territory, Canada. Arctic 51, 105–115.
Burn, C.R., 1997. Cryostratigraphy, paleogeography, and climate change during the early Holocene warm interval, western Arctic coast, Canada. Canadian Journal of Earth Sciences 34, 912–925.
Cardyn, R., Clark, I.D., Lacelle, D., Lauriol, B., Zdanowicz, C., Calmels, F., 2007. Molar gas ratios of air entrapped in ice: a new tool to determine the nature and origin of relict massive ground ice bodies in permafrost. Quaternary Research 68, 239–248.
Catto, N.R., 1986. Quaternary sedimentology and stratigraphy, Peel Plateau and Richardson Mountains, Yukon and Northwest Territories. (Unpublished Ph.D. thesis) Department of Geology, University of Alberta (728 pp.).
Catto, N.R., 1996. Richardson Mountains, Yukon-Northwest Territories: the northern portal of the postulated "ice-free corridor". Quaternary International 32, 3–19.
Clark, I.D., Lauriol, B., 1997. Aufeis of the Firth River basin, northern Yukon, Canada: insights into permafrost hydrogeology and karst. Arctic and Alpine Research 29, 240–252.
Clark, P.U., Dyke, A.S., Shakun, J.D., Carlson, A.E., Clark, J., Wohlfarth, B., Mitrovica, J.X., Hostetler, S.W., McCabe, A.M., 2009. The Last Glacial Maximum. Science 325 (5941), 710–714.
Coplen, T.B., Kendall, C., Hopple, J., 1983. Comparison of isotope reference samples. Nature 302, 236.
Duk-Rodkin, A., Hughes, O.L., 1991. Age relationships of Laurentide and Montane glaciations, Mackenzie Mountains, Northwest Territories. Geographie Physique et Quaternaire 45, 79–90.
Duk-Rodkin, A., Hughes, O.L., 1992. Surficial geology, Fort McPherson-Bell River. Yukon-Northwest Territories. Geological Survey of Canada, Map 1745A, scale 1:250 000.
Duk-Rodkin, A., Hughes, O.L., 1995. Quaternary geology of the northeastern part of the central Mackenzie Valley Corridor, District of Mackenzie, Northwest Territories. Geological Survey of Canada, Bulletin 458 (45 pp.).
Duk-Rodkin, A., Lemmen, D.S., 2000. Glacial history of the Mackenzie region. In: Dyke, L.D., Brooks, G.R. (Eds.), The Physical Environment of the Mackenzie Valley, Northwest Terrotories: a Base Line for the Assessment of Environmental Change: Geological Survey of Canada, Bulletin, 547, pp. 11–20.
Duk-Rodkin, A., Barendregt, R.W., Tarnocai, C., Phillips, F.M., 1996. Late Tertiary to Late Quaternary record in the Mackenzie Mountains, Northwest Territories, Canada: stratigraphy, paleomagnetism, and chlorine-36. Canadian Journal of Earth Sciences 33, 875–895.
Dyke, A.S., Andrews, J.T., Clark, P.U., England, J.H., Miller, G.H., Shaw, J., Veillette, J., 2002. The Laurentide and Innuitian ice sheets during the Last Glacial Maximum. Quaternary Science Reviews 21, 9–31.
England, J.H., Furze, M.F.A., Doupé, J.P., 2009. Revision of the NW Laurentide Ice Sheet: implications for paleoclimate, the northeast extremity of Beringia, and the Arctic Ocean sedimentation. Quaternary Science Reviews 28, 1573–1596.
Fritz, M., Herzschuh, U., Wetterich, S., Lantuit, H., De Pascale, G.P., Pollard, W.H., Schirmeister, L., 2012. Late glacial and Holocene sedimentation, vegetation, and climate history from easternmost Beringia (northern Yukon Territory, Canada). Quaternary Research 78, 549–560.
Froese, D.G., Zazula, G.D., Reyes, A.V., 2006. Seasonality of the late Pleistocene Dawson tephra and exceptional preservation of a buried riparian surface in central Yukon Territory, Canada. Quaternary Science Reviews 25, 1542–1551.
Guthrie, R.D., Stoker, S., 1990. Paleoecological significance of mummified remains of Pleistocene horses from the North Slope of the Brooks Range, Alaska. Arctic 43, 267–274.
Hall, D.K., 1980. Mineral precipitation in North Slope river icings. Arctic 33, 343–348.
Harington, C.R., 1990. Ice Age Vertebrates in the Canadian Arctic Islands. Canada's Missing Dimension Vol. 1. Canadian Museum of Nature, Ottawa, pp. 138–160.
Harington, C.R., Cinq-Mars, J., 1995. Radiocarbon dates on saiga antelope (*Saiga tatarica*) fossils from Yukon and the Northwest Territories. Arctic 48, 1–7.
Hillaire-Marcel, C., Causse, C., 1989. The Late Pleistocene Laurentide Glacier: Th/U dating of its major fluctuations and $\delta^{18}O$ range of the ice. Quaternary Research 32, 125–138.
Hopkins, D.M., Smith, P.A., 1981. Dated wood from Alaska and Yukon: implications for forest refugia in Beringia. Quaternary Research 15, 217–249.
Hughes, O.L., 1972. Surficial geology of northern Yukon Territory and northwestern District of Mackenzie, Northwest Territories. Geological Survey of Canada Paper 69–36 (11 pp.).
Hughes, O.L., Harington, C.R., Janssens, J.A., Matthews, J.V., Morlan, R.E., Rutter, N.W., Schweger, C.E., 1981. Upper Pleistocene stratigraphy, paleoecology and archeology of northern Yukon interior, eastern Beringia 1. Bonnet Plume Basin. Arctic 34, 329–365.
Kaufman, D.S., et al., 2004. Holocene thermal maximum in the western Arctic (0–180°W). Quaternary Science Reviews 23, 529–560.

https://doi.org/10.1016/j.yqres.2013.06.001 Published online by Cambridge University Press

Kennedy, K.E., Froese, D.G., Zazula, G.D., Lauriol, B., 2010. Last Glacial Maximum age for the northwest Laurentide maximum from the Eagle River spillway and braid delta complex, northern Yukon. Quaternary Science Reviews 29, 1288–1300.
Lacelle, D., 2007. Environmental setting, (micro)morphologies and stable C–O isotope composition of cold carbonate precipitates — a review and evaluation of their potential as paleoclimate proxies. Quaternary Science Reviews 26, 1670–1689.
Lacelle, D., 2011. On the $\delta^{18}O$, δD and D-excess relations in meteoric precipitation and during equilibrium freezing: theoretical approach and field examples. Permafrost and Periglacial Processes 22, 13–25.
Lacelle, D., Bjornson, J., Lauriol, B., Clark, I.D., Troutet, Y., 2004. Segregated-intrusive ice of subglacial meltwater origin in retrogressive thaw-flow headwalls, Richardson Mountains, NWT, Canada. Quaternary Sciences Reviews 23, 681–696.
Lacelle, D., Lauriol, B., Clark, I.D., 2006. Effect of chemical of water on the oxygen-18 and carbon-13 signature preserved in cryogenic carbonates, Arctic Canada: Implications in paleoclimatic studies. Chemical Geology 234, 1–16.
Lauriol, B., Cinq-Mars, J., Clark, I.D., 1991. Les naleds du nord Yukon: localisation, genèse et fonte. Permafrost and Periglacial Processes 2, 225–236.
Lauriol, B., Lacelle, D., St-Jean, M., Clark, I.D., Zazula, G.D., 2010. Late Quaternary paleoenvironments and growth of intrusive ice in eastern Beringia (Eagle River valley, northern Yukon, Canada). Canadian Journal of Earth Sciences 47, 941–955.
Lemmen, D.S., Duk-Rodkin, A., Bednarski, J.M., 1994. Late glacial drainage systems along the northwestern margin of the Laurentide Ice Sheet. Quaternary Science Reviews 13, 805–828.
Michel, F., 2011. Isotope characterisation of ground ice in northern Canada. Permafrost and Periglacial Processes 22, 3–12.
Moorman, B.J., Michel, F.A., 2000. The burial of ice in the proglacial environment on Bylot Island, Arctic Canada. Permafrost and Periglacial Processes 11, 161–175.
Morlan, R.E., 1986. Pleistocene archaeology in Old Crow basin: a critical reappraisal. In: Bryan, A.L. (Ed.), New Evidence for the Pleistocene Peopling of the Americas, University of Maine. Center for the Study of Early Man, Orono, pp. 27–48.
Murton, J.B., Frenchen, M., Maddy, D., 2007. Luminescence dating of mid- to Late Wisconsinan aeolian sand as a constraint on the last advance of the Laurentide Ice Sheet across the Tuktoyaktuk Coastlands, western Arctic Canada. Canadian Journal of Earth Sciences 44, 857–869.
Norris, D. K., 1985. Geology of the northern Yukon and northwestern District of Mackenzie. Geological Survey of Canada, map 1581A, scale 1:500,000.
Pollard, W.H., 2005. Icing processes associated with High Arctic perennial springs, Axel Heiberg Island, Nunavut, Canada. Permafrost and Periglacial Processes 16, 51–68.
Rampton, V.N., 1982. Quaternary Geology of the Yukon Coastal Plain. Geological Survey of Canada, Bulletin 317 (49 pp.).
Refsnider, K.A., Miller, G.H., Hillaire-Marcel, C., Fogel, M.L., Ghaleb, B., Bowden, R., 2012. Subglacial carbonates constrain basal conditions and oxygen isotopic composition of the Laurentide Ice Sheet over Arctic Canada. Geology 40, 135–138.
Reimer, P.J., Baillie, M.G.L., Bard, E., Bayliss, A., Beck, J.W., Blackwell, P.G., Bronk Ramsey, C., Buck, C.E., Burr, G.S., Edwards, R.L., Friedrich, M., Grootes, P.M., Guilderson, T.P., Hajdas, I., Heaton, T.J., Hogg, A.G., Hughen, K.A., Kaiser, K.F., Kromer, B., McCormac, F.G., Manning, S.W., Reimer, R.W., Richards, D.A., Southon, J.R., Talamo, S., Turney, C.S.M., van der Plicht, J., Weyhenmeyer, C.E., 2009. IntCal09 and Marine09 radiocarbon age calibration curves, 0–50,000 years cal BP. Radiocarbon 51 (4), 1111–1150.
Schweger, C.E., Matthews, J.V., 1991. The last (Koy-Yukon) interglaciation in the Yukon: comparison with Holocene and interstadial pollen records. Quaternary International 10–12, 85–94.
St-Jean, M., Lauriol, B., Clark, I.D., Lacelle, D., Zdanowicz, C., 2011. Understanding the filling process in ice wedges using crystallography, stable O–H isotopes and gas composition (O2, N2, Ar). Permafrost and Periglacial Processes 22, 49–64.
Utting, N., 2010. Geochemistry and noble gases of permafrost groundwater and ground ice in Yukon and the Northwest Territories, Canada. (Unpublished PhD thesis) University of Ottawa, Ottawa, Canada.
Vincent, J.-S., 1989. Quaternary geology of the northern Canadian Interior Plains. In: Fulton, R.J. (Ed.), Quaternary Geology of Canada and Greenland, 1: Geological Survey of Canada, Geology of Canada, pp. 100–137.
Vincent, J.S., Hardy, L., 1979. The evolution of glacial lakes Barlow and Ojibway, Québec and Ontario. Geological Survey of Canada, Bulletin 316 (18 pp.).
Zazula, G.D., Duk-Rodkin, A., Schweger, C.E., Morlan, R.E., 2004. Late Pleistocene chronology of glacial Lake Old Crow and the north-west margin of the Laurentide Ice Sheet. In: Ehlers, J., Gibbard, P.L. (Eds.), Quaternary Glaciations — Extent and Chronology, Part II, pp. 347–362.
Zazula, G.D., Hare, P.G., Storer, J.E., 2009a. New radiocarbon dated vertebrate fossils from Herschel Island: implications for the glacial chronology and palaeoenvironments of the Beaufort Sea Coastlands. Arctic 62, 273–280.
Zazula, G.D., Mackay, G., Andrews, T.D., Shapiro, B., Letts, B., Brock, F., 2009b. A Late Pleistocene steppe bison (*Bison priscus*) partial carcass from Tsiigehtchic, Northwest Territories, Canada. Quaternary Science Reviews 28, 2734–2742.

https://doi.org/10.1016/j.yqres.2013.06.001 Published online by Cambridge University Press